

POLARIZATION OBSERVATIONS OF THE ANOMALOUS MICROWAVE EMISSION IN THE PERSEUS MOLECULAR COMPLEX WITH THE COSMOSOMAS EXPERIMENT

E. S. BATTISTELLI,^{1,2} R. REBOLO,^{1,3} J. A. RUBIÑO-MARTÍN,¹ S. R. HILDEBRANDT,¹ R. A. WATSON,^{1,4}
 C. GUTIÉRREZ,¹ AND R. J. HOYLAND¹

Received 2006 March 14; accepted 2006 May 26; published 2006 July 6

ABSTRACT

The anomalous microwave emission detected in the Perseus molecular complex by Watson et al. has been observed at 11 GHz through dual orthogonal polarizations with the COSMOSOMAS experiment. Stokes U and Q maps were obtained at a resolution of $\sim 0.9''$ for a $30'' \times 30''$ region including the Perseus molecular complex. Faint polarized emission has been measured; we find $Q = -0.2\% \pm 1.0\%$ and $U = -3.4^{+1.8}_{-1.4}\%$, both at the 95% confidence level, with a systematic uncertainty estimated to be lower than 1% determined from tests of the instrumental performance using unpolarized sources in our map as null hypothesis. The resulting total polarization level is $\Pi = 3.4^{+1.5}_{-1.9}\%$. These are the first constraints on the polarization properties of an anomalous microwave emission source. The low level of polarization seems to indicate that the particles responsible for this emission in the Perseus molecular complex are not significantly aligned in a common direction over the whole region, as a consequence of either a high structural symmetry in the emitting particle or a low-intensity magnetic field. Our weak detection is fully consistent with predictions from electric dipole emission and resonance relaxation at this frequency.

Subject headings: diffuse radiation — dust, extinction — ISM: individual (G159.6–18.5) — polarization — radio continuum: ISM — radiation mechanisms: general

1. INTRODUCTION

Since the *Cosmic Background Explorer* (COBE) first detected dust-correlated microwave emission in its maps (Kogut et al. 1996), a significant effort has been made by the scientific community to understand the origin of this anomalous emission and characterize its properties. Further statistical evidence has been found in observations and analysis by Leitch et al. (1997), de Oliveira-Costa et al. (1997, 1998, 1999, 2002, 2004), Mukherjee et al. (2001, 2003), Lagache et al. (2003), Finkbeiner (2004), Finkbeiner et al. (2004), and Davies et al. (2005). Still, the underlying mechanism for this emission is a matter of discussion due to the lack of measurements about its properties, and different models have been proposed to explain its observed characteristics.

The COSMOSOMAS experiment⁵ of the Instituto de Astrofísica de Canarias (IAC) is now able to provide frequency and sky coverage needed to increase our understanding of the statistical and physical properties of the anomalous microwave emission (Fernández-Cerezo et al. 2006; S. Hildebrandt et al. 2006, in preparation). Watson et al. (2005, hereafter W05) have recently presented a direct detection of rising-spectrum emission by COSMOSOMAS in the Perseus molecular cloud (R.A. = $55^{\circ}4$, decl. = $31^{\circ}8$; J2000) that is an order of magnitude higher than what can be explained with standard Galactic mechanisms of emission (i.e., free-free, synchrotron, and thermal dust) and which cannot be explained with ultracompact H II regions or a gigahertz-peaked source. In this Letter, we present polarization measurements of this anomalous emission per-

formed with the COSMOSOMAS experiment. It is worth stressing that the W05 detection refers to an extended region that appears diffuse even at the COSMOSOMAS angular resolution ($\sim 1''$) with a Gaussian FWHM fit over the emitting region of $\sim 2''$. Our polarization measurements are characterized by the same angular resolution.

2. ANOMALOUS MICROWAVE EMISSION: INTERPRETATION AND POLARIZATION PROPERTIES

Comparisons between anomalous-emission detections and H α maps have already ruled out the possibility that the statistical and direct observations are due to free-free emission from ionized gas (see, e.g., Draine & Lazarian 1998a, 1998b). Ultracompact H II regions have also been invoked by McCullough & Chen (2002) to explain the direct tentative detection obtained by Finkbeiner et al. (2002) as the superposition of a compact, optically thick and an extended, optically thin H II region, both being free-free emitters. Bremsstrahlung emission is intrinsically unpolarized, although polarization may occur by means of Thomson scattering when photons are rescattered within an H II region. This may occur in optically thick regions, where the level of polarization can be at most 10% (Keating et al. 1998). Bennett et al. (2003a, 2003b) and Hinshaw et al. (2006) interpret the dust-correlated component as synchrotron emission with a flatter spectral index. However, the results of the Tenerife Experiment (e.g., de Oliveira-Costa et al. 2004) and the analysis of Lagache (2003) are not consistent with this interpretation. In any case, polarization measurements are essential to probe this hypothesis, because the synchrotron emission is expected to be highly polarized.

Draine & Lazarian (1998a, 1998b) have proposed that the anomalous dust-correlated emission is due to electric dipole emission from rapidly rotating small dust grains (i.e., “spinning dust”) in the interstellar medium. They have delved into the details of the mechanisms of excitation and damping and concluded that their emission spectrum may fit well the observed signal and be responsible for this anomalous emission. Lazarian

¹ Instituto de Astrofísica de Canarias, Calle Vía Láctea s/n, E-38205 La Laguna, Tenerife, Spain.

² Current address: Department of Physics and Astronomy, University of British Columbia, 6224 Agricultural Road, Vancouver, BC V6T 1Z1, Canada; elia@phas.ubc.ca.

³ Consejo Superior de Investigaciones Científicas, Spain.

⁴ Jodrell Bank Observatory, University of Manchester, Macclesfield, Cheshire SK11 9DL, UK.

⁵ See <http://www.iac.es/project/cmb/cosmosomas>.

& Draine (2000) continued the study of spinning dust grains in the presence of weak magnetic fields and found that paramagnetic relaxation resonance, in a domain where classical paramagnetic relaxation is suppressed, may be efficient at producing an alignment of grains rotating faster than 1 GHz. This may result in the presence of an observable polarization as high as 5% at 10 GHz that rapidly decreases at higher frequencies, in the anomalous emission, depending on the phase in the sky of the magnetic field. Still, the level of alignment depends on factors such as the efficiency of spin-lattice relaxation, which is uncertain for very small grains ($<10^{-7}$ cm).

Magnetic dipole emission from dust grains has also been found to be of considerable interest at frequencies below 100 GHz. Draine & Lazarian (1999) calculated the spectra of different grain candidates and found that ordinary paramagnetic grains exhibit emission spectra that are noticeably different from the observed anomalous emission. However, they proposed a model, adjusting the magnetic properties of the emitting material, that involves strong magnetic material whose emission may account, at least in part, for the observed anomalous emission. For this model, ferromagnetic relaxation may efficiently act to align dust grains and produce strongly frequency- and shape-dependent polarized emission that could be as high as 30% at 10 GHz. A key signature of polarized emission from a magnetic dipole, with respect to an electric dipole, is the variation of its direction with frequency.

We note that both electric and magnetic dipole emissions are model dependent, making it difficult to effectively predict their polarization properties. However, according to the model proposed by Draine & Lazarian (1999), in order to account for the observed spectrum, a hypothetical material “X4” characterized by strong magnetic grains has to be considered. Therefore, asymmetric grains will be aligned even by a low-intensity magnetic field like the Galactic field, resulting in both a higher polarization level and a higher probability for alignment to occur with respect to electric dipole emission.

Iglesias-Groth (2005, 2006) studied the rotation rates of hydrogenated fullerenes and electric dipole emission in the interstellar medium and found that the smallest of these molecules could be the origin of the anomalous emission detected by W05 in the Perseus molecular complex and by Casassus et al. (2006) in the dark cloud LDN 1622. In addition, weak ferromagnetic properties exhibited by some of these molecules may lead to a consistent alignment and consequently to detectable polarization.

3. COSMOSOMAS OBSERVATIONS

3.1. The Instrument

The COSMOSOMAS experiment is located at the Teide Observatory, at 2400 m above sea level in Tenerife (Spain). It comprises two circular-scanning instruments and generates two daily maps at 11 GHz (COSMO11 instrument) and three maps at 13, 15, and 16 GHz (COSMO15 instrument). The angular resolution is approximately $0''.9$. The interested reader may refer to Gallegos et al. (2001) for a general description of the COSMO15 instrument and the adopted observational strategy. COSMO11 has a similar instrumental setup to that of COSMO15. The optical configuration is identical (dimensions are scaled with wavelength), with a rotating primary flat mirror and a secondary parabolic mirror focusing the radiation into a cryogenically cooled receiver. The detectors are low-noise HEMT amplifiers cooled to 20 K.

The main difference between the two experiments is that COSMO11 is optimized for polarization measurements. An ortho-mode transducer is used to separate two orthogonal polarizations after the radiation collector and before the HEMT, which are followed by further amplification stages. This configuration allows one to sample the sky and perform measurements of two Stokes parameters at a time: I and Q (or U , depending on the orientation in the sky of the measured polarization planes). In order to completely characterize the linear polarization of the measured emission, the sampled polarization planes can be rotated by 45° by simply rotating the front end of the experiment, allowing one to switch the receiver sensitivity from Q to U (and vice versa). A detailed description of the instrument will be presented in R. Hoyland et al. (2006, in preparation).

3.2. Data Analysis

COSMO11 creates daily maps with full coverage in right ascension and $\sim 20^\circ$ coverage in declination. Raw data are stacked in scan collections in which the detected data, resulting from the adopted circular scan strategy, are saved as a function of time. Each scan is the result of an average over 30 cycles (equivalent to 30 s). Atmospheric emission is evident in the scans as a pseudosinusoidal modulation due to changing air masses within the circles covered on the sky by the instrument. This modulation has been removed by calculating a template and subtracting it from our scans. The template was calculated by averaging over 2 hr, masking bright sources and the Galactic plane, and iterating the procedure. The time over which the template was calculated was chosen by considering the final signal-to-noise ratio as a function of time. This procedure allows the subtraction of slow day-night modulation, including $1/f$ noise as well as other fixed systematics such as optical pickup, which are in any event strongly reduced by under-illuminating the primary mirror. We note that this data processing differs from that adopted in W05, and by Fernández-Cerezo et al. (2006), and is aimed at preserving the large scales of the emission (i.e., to extend the window function to lower multipoles l). After the cleaning procedure, we proceed to the projection of the scans into the sky map, using bright sources to check for consistency in the pointing reconstruction. The final pixelization is $\frac{1}{3}^\circ \times \frac{1}{3}^\circ$. After that, we sum the daily maps into cumulated maps. The main calibration is performed with Cygnus A on a daily basis. Absolute flux is taken from the model by Baars et al. (1977). The instrumental beam is also calculated using the main calibrator for each day. The overall beam is recalculated using the cumulated map, and afterward we recalibrate all the maps with fixed FWHMs with Gaussian fits over the calibration source.

In calculating the source emission, we take great care to account for contamination that might be due to the Sun or the Moon in the proximity of the target sources. We have adopted a conservative attitude, removing from the analysis those data in which the Sun is closer than $\sim 30^\circ$ to the regions of interest. Our conservative attitude originates from concern about possible (even very low) asymmetric pickup resulting in a polarized signal. A significant effort has been made to track the instrument's stability using radio sources and H II region emission and polarization with time. Among other sources, we have checked in the reconstructed map the coordinates of 4C 39.25 and 3C 345 outside the Galactic plane, and 3C 84 and IC 405 in the Galactic anticenter, close to the Perseus region of interest.

These sources have allowed us to test possible effects arising from the distance to the calibration source in our maps, and to check that possible misalignment effects in the optical system of the instrument are not affecting the local reconstruction of the microwave sky in the region of interest. Also, the relatively close H II region NGC 1499 (the California Nebula) has been used to test for possible effects and systematics arising from measurements of extended sources compared with pointlike sources. All of these sources have shown a good level of stability or slow variation compatible with intrinsic flux variations. NGC 1499 has also been carefully studied to check for spurious effects and as a null hypothesis test, since diffuse H II regions are expected to mainly emit free-free radiation, which is intrinsically unpolarized.

Possible diffuse polarized synchrotron emission has been checked using the maps from Wolleben et al. (2006).⁶ Wolleben et al. point out the presence of depolarized regions around H II regions. Fortunately, this does not have an effect on the polarized emission of the Perseus molecular cloud, which is known to be closer to us than NGC 1499. A detailed analysis of the Wolleben et al. polarization maps, and the extrapolation toward COSMOSOMAS frequencies, shows possible residual polarized signal lower than 1% in the NGC 1499 region, even assuming a spectral index as high as -2.7 . We thus finally recalibrated our Perseus emission with NGC 1499.

The coordinate convention adopted in this Letter to define the Q and U Stokes parameters is as follows: At every point on sky, the X -axis points north, and the Y -axis points east. In the first COSMO11 configuration, we measure I_0 (intensity along the X -axis) and I_{90} (intensity along the Y -axis), while in the second orientation of the system we obtain I_{+45} and I_{-45} . Our definition of the Stokes parameters is $Q = I_0 - I_{90}$ and $U = I_{+45} - I_{-45}$. For each of the two configurations, we have two determinations of the intensity, which we denote as $I_Q = I_0 + I_{90}$ and $I_U = I_{+45} + I_{-45}$. Finally, the total polarization degree is defined as $\Pi = (Q^2 + U^2)^{1/2}/I$.

Spurious instrumental polarization induced by oblique reflections in our off-axis system has been calculated, in a regime of ordinary skin effect, using the method presented by Renbarger et al. (1998), and found to be totally negligible compared with other systematics. The two channels have almost identical spectral response, resulting in a negligible systematic effect arising from the passband mismatch between observed calibrator and the Perseus region (i.e., the effect is canceled out). Further instrumental effects have been tested for by rotating the front end of the instrument by 90° and checking for consistency.

Measurements of Q were taken over the period between 2004 March and 2005 May, while measurements of U are extracted from the measurements performed after this month. The time coverage is not uniform, as a result of contamination, variation in the atmospheric conditions, and instrumental failures, which have been reduced to a minimum thanks to continuous monitoring of the instrument's performance. The integration time for the U -measurements is smaller than that for Q , resulting in higher statistical errors. The residual systematics are monitored by measurements of NGC 1499, using this H II region as a null test. This is done in two steps: by directly observing NGC 1499 on the Cygnus-calibrated map, and then by considering the possibility of a faint polarization of the main calibrator, which could result in an apparent polarization signal of the

H II region. Tests on the Wolleben et al. (2006) maps allowed us to check for this possibility and, after accounting for this, to constrain the systematics for both the Q - and U -directions at a lower level than the statistical uncertainties. In order to double-check this result we have carefully monitored 3C 84, whose emission is expected to be variable with time but whose polarization is expected to be far below 1%.⁷ We find a final polarization level lower than 1%, which sets our systematics level.

4. RESULTS AND DISCUSSION

The effective polarized emission from the Perseus region has been calculated through a maximum likelihood analysis using the measurements of the partial stacked maps. This likelihood was built using a multivariate Gaussian distribution. Measurements at different epochs were assumed to be uncorrelated, so the covariance matrix in this case is diagonal. We describe the data with a two-parameter model, one for the value (assumed to be constant in time) for the polarization of the Perseus region, and another for the calibration uncertainty. This latter parameter is marginalized over by following the analytical prescription given by Bridle et al. (2002), assuming a Gaussian prior for its value with 10% width (overall calibration uncertainty). Note that in the case of the fractional polarization, the calibration uncertainty does not enter. Once the likelihood curves are computed, the confidence limits are derived from the 0.025, 0.5, and 0.975 points of the cumulative distribution function. Thus, our parameter estimate is the median of the marginalized posterior probability distribution function, and the confidence interval encompasses 95% of the probability. In Figure 1, we present the map of the Perseus region emission and the two difference maps of 90° polarization orientation describing the Q and U parameters.

We find a small polarization in both orientations: for the $0^\circ/90^\circ$ orientation we obtain $Q/I = -0.2\% \pm 1.0\%$, while for the $45^\circ/-45^\circ$ one we have $U/I = -3.4^{+1.8}_{-1.4}\%$, both at the 95% confidence level, for a total polarization of $\Pi = 3.4^{+1.5}_{-1.9}\%$. The polarization in the $0^\circ/90^\circ$ orientation is thus consistent with a null measurement within the systematic and statistical uncertainties. A polarization in U is possible, both from a statistical and a systematic point of view. From the considerations highlighted in § 1, although model-dependent uncertainties are widely present, the low level of polarization in the Perseus anomalous emission appears to be inconsistent with magnetic dipole emission of highly oriented particles in the presence of a magnetic field, either because of low field intensity in the region, or because of the highly symmetric nature of the emitting particles. Our results favor electric dipole emission as being responsible, the emission properties of which are even more model dependent but whose polarization is limited to $\sim 5\%$. In particular, as described by Lazarian & Draine (2000), paramagnetic relaxation resonance may produce an observable polarized signal of the same order as that observed by COSMOSOMAS for an equivalent grain radius of $\lesssim 10^{-7}$ cm. Our observations are limited both by the interpretation of the models and by our angular resolution. In fact, we cannot constrain magnetically emitting grains characterized by weak magnetic properties or by spherical shape, and we cannot monitor structures characterized by angular dimensions smaller than our angular resolution in the observed region. This latter problem

⁶ See <http://www.drao-ofr.hia-ih.nrc-cnrc.gc.ca/26msurvey/data.html>.

⁷ See the UMRAO database, at <http://www.astro.lsa.umich.edu>.

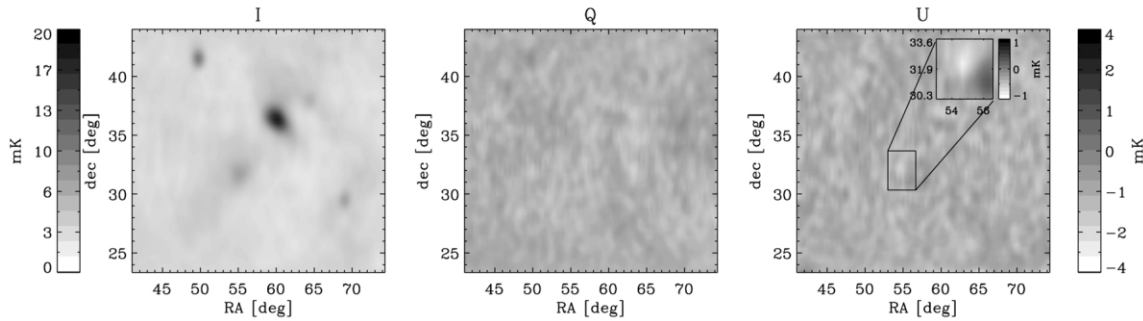


FIG. 1.—Stokes I , Q , and U COSMOSOMAS 11 GHz maps of the region around the Perseus molecular complex. In the I map, the brightest source is the NGC 1499 H II region. The fainter source at R.A. = 55°4, decl. = 31°8 (J2000) is the observed (anomalously) emitting region. The source 3C 84 is also visible in the intensity map, with coordinates R.A. = 49°9, decl. = 41°5. The (gray scale) color bar on the left refers to the I map, while that on the right refers to both Q and U maps. The maps have been smoothed with a 3 pixel boxcar. The inset in the U map refers to the faint detection achieved in the Perseus molecular complex.

is, however, somewhat lessened by the fact that the measurement from W05 is over an extended region, and so we expect anomalous-emission properties to characterize the entire region. Further polarization observations with higher sensitivity and angular resolution, as well as monitoring other frequencies of interest for the anomalous emission, will further help in understanding the mechanism responsible for this emission.

5. CONCLUSIONS

We have observed the Perseus molecular cloud in order to extract information about the polarization properties of the anomalous microwave emission observed by W05. A careful analysis and control of systematics lead us to the conclusion that this emission is characterized by a low level of polarization: $\Pi = 3.4^{+1.5}_{-1.9}\%$ at 95% confidence, with systematic uncertainties limited to 1%. To infer the real emission mechanism for the anomalous emission, local physical properties of the observed

regions should be further investigated. However, the weak detected polarization seems to support the electric dipole emission model, with resonance relaxation, over the dipole magnetic emission hypothesis. Further information about the effective origin of this emission will be available with higher resolution, higher sensitivity, multifrequency observations already planned at the Teide Observatory and, we hope, to be planned for other instruments.

We acknowledge the support of the IAC and the staff of Teide Observatory for the construction and operation of the COSMOSOMAS experiment. Partial funding was provided by grant AYA 2001-1657 from the Spanish Ministry of Science and Education. We thank M. Wolleben for the online 1.4 GHz maps. We thank E. Chapin for useful comments and for revising the English. Also, we would like to thank the referee for useful comments that allowed us to improve this Letter.

REFERENCES

- Baars, J. W. M., Genzel, R., Pauliny-Toth, I. I. K., & Witzel, A. 1977, *A&A*, 61, 99
- Bennett, C. L., et al. 2003a, *ApJS*, 148, 1
- . 2003b, *ApJS*, 148, 97
- Bridle, S. L., Crittenden, R., Melchiorri, A., Hobson, M. P., Kneissl, R., & Lasenby, A. N. 2002, *MNRAS*, 335, 1193
- Casassus, S., Cabrera, G. F., Förster, F., Pearson, T. J., Readhead, A. C. S., & Dickinson, C. 2006, *ApJ*, 639, 951
- Davies, R. D., Dickinson, C., Banday, A. J., Jaffe, T. R., Górski, K. M., & Davis, R. J. 2005, *MNRAS*, submitted (astro-ph/0511384)
- de Oliveira-Costa, A., Kogut, A., Devlin, M. J., Netterfield, C. B., Page, L. A., & Wollack, E. J. 1997, *ApJ*, 482, L17
- de Oliveira-Costa, A., Tegmark, M., Davies, R. D., Gutiérrez, C. M., Lasenby, A. N., Rebolo, R., & Watson, R. A. 2004, *ApJ*, 606, L89
- de Oliveira-Costa, A., Tegmark, M., Gutiérrez, C. M., Jones, A. W., Davies, R. D., Lasenby, A. N., Rebolo, R., & Watson, R. A. 1999, *ApJ*, 527, L9
- de Oliveira-Costa, A., Tegmark, M., Page, L. A., & Boughn, S. P. 1998, *ApJ*, 509, L9
- de Oliveira-Costa, A., et al. 2002, *ApJ*, 567, 363
- Draine, B. T., & Lazarian, A. 1998a, *ApJ*, 494, L19
- . 1998b, *ApJ*, 508, 157
- . 1999, *ApJ*, 512, 740
- Fernández-Cerezo, S., et al. 2006, *MNRAS*, in press
- Finkbeiner, D. P. 2004, *ApJ*, 614, 186
- Finkbeiner, D. P., Langston, G. I., & Minter, A. H. 2004, *ApJ*, 617, 350
- Finkbeiner, D. P., Schlegel, D. J., Frank, C., & Heiles, C. 2002, *ApJ*, 566, 898
- Gallegos, J. E., Macías-Pérez, J. F., Gutiérrez, C. M., Rebolo, R., Watson, R. A., Hoyland, R. J., & Fernández-Cerezo, S. 2001, *MNRAS*, 327, 1178
- Hinshaw, G., et al. 2006, *ApJ*, submitted (astro-ph/0603451)
- Iglesias-Groth, S. 2005, *ApJ*, 632, L25
- . 2006, *MNRAS*, 368, 1925
- Keating, B., Timbie, P., Polnarev, A., & Steinberger, J. 1998, *ApJ*, 495, 580
- Kogut, A., Banday, A. J., Bennett, C. L., Górski, K. M., Hinshaw, G., Smoot, G. F., & Wright, E. L. 1996, *ApJ*, 464, L5
- Lagache, G. 2003, *A&A*, 405, 813
- Lazarian, A., & Draine, B. T. 2000, *ApJ*, 536, L15
- Leitch, E. M., Readhead, A. C. S., Pearson, T. J., & Myers, S. T. 1997, *ApJ*, 486, L23
- McCullough, P. R., & Chen, R. R. 2002, *ApJ*, 566, L45
- Mukherjee, P., Coble, K., Dragovan, M., Ganga, K., Kovac, J., Ratna, B., & Souradeep, T. 2003, *ApJ*, 592, 692
- Mukherjee, P., Jones, A. W., Kneissl, R., & Lasenby, A. N. 2001, *MNRAS*, 320, 224
- Renbarger, T., Dotson, J. L., & Novak, G. 1998, *Appl. Opt.*, 37, 6643
- Watson, R. A., Rebolo, R., Rubiño-Martín, J. A., Hildebrandt, S., Gutiérrez, C. M., Fernández-Cerezo, S., Hoyland, R. J., & Battistelli, E. S. 2005, *ApJ*, 624, L89 (W05)
- Wolleben, M., Landecker, T. L., Reich, W., & Wielebinski, R. 2006, *A&A*, 448, 411